

2,3-Dihydroxyisovalerate production by *Klebsiella pneumoniae*

Yike Wang<sup>1,3,4,#</sup>, Jinjie Gu<sup>1,5,#</sup>, Xiyang Lu<sup>1</sup>, Zhongxi Zhang<sup>1,3</sup>, Yang Yang<sup>1,3,4</sup>, Shaoqi Sun<sup>1,3,4</sup>, Emily T. Kostas<sup>2</sup>, Jiping Shi<sup>1,5</sup>, Mintian Gao<sup>3</sup>, Frank Baganz<sup>2\*</sup>, Gary J. Lye<sup>2\*</sup>, Jian Hao<sup>1,2\*</sup>

1. Lab of Biorefinery, Shanghai Advanced Research Institute, Chinese Academy of Sciences, No. 99 Haike Road, Pudong, Shanghai, 201210, PR China

2. Department of Biochemical Engineering, University College London, Gordon Street, London WC1H 0AH, UK

3. School of Life Science, Shanghai University, Shanghai 200444, PR China

4. University of Chinese Academy of Sciences, Beijing, 100049, PR China

5. School of life science and technology, ShanghaiTech University

# Both authors contributed equally to this work

\*Corresponding author.

Email: haoj@sari.ac.cn

g.lye@ucl.ac.uk

f.baganz@ucl.ac.uk

Tel.: +86 21 20325163

17

18 **Abstract**

19 2,3-Dihydroxyisovalerate is an intermediate of valine and leucine biosynthesis pathway, however, no  
20 natural microorganism has been found yet that can accumulate this compound. *Klebsiella pneumoniae* is  
21 a useful bacterium that can be used as a workhorse for the production of a range of industrially desirable  
22 chemicals. Dihydroxy acid dehydratase, encoded by the *ilvD* gene, catalyses the reaction of 2-  
23 ketoisovalerate formation from 2,3-dihydroxyisovalerate. In this study, an *ilvD* disrupted strain was  
24 constructed which resulted in the inability to synthesize 2-ketoisovalerate, yet accumulate 2,3-  
25 dihydroxyisovalerate in its culture broth. 2,3-Butanediol is the main metabolite of *K. pneumoniae* and its  
26 synthesis pathway and the branched-chain amino acid synthesis pathway share the same step of the  $\alpha$ -  
27 acetolactate synthesis. By knocking out the *budA* gene, carbon flow into the branched-chain amino acid  
28 synthesis pathway was upregulated which resulted in a distinct increase in 2,3-dihydroxyisovalerate  
29 levels. Lactic acid was identified as a by-product of the process and by blocking the lactic acid synthesis  
30 pathway a further increase in 2,3-dihydroxyisovalerate levels was obtained. The culture parameters of  
31 2,3-dihydroxyisovalerate fermentation were optimized, which include acidic pH and medium level  
32 oxygen supplementation to favor 2,3-dihydroxyisovalerate synthesis. At optimal conditions (pH 6.5, 400  
33 rpm), 36.5 g/L of 2,3-dihydroxyisovalerate was produced in fed-batch fermentation over 45 hours, with  
34 a conversion ratio of 0.49 mol/mol glucose. Thus a biological route of 2,3-dihydroxyisovalerate  
35 production with high conversion ratio and final titer was developed; providing a basis for an industrial  
36 process.

37

38 **Key words:** 2,3-Dihydroxyisovalerate; 2,3-Butanediol; 2-Ketoisovalerate; *Klebsiella pneumoniae*; *ilvD*

39

## 40 Introduction

41 *Klebsiella pneumoniae* is a Gram-negative bacterium that is ubiquitous in the natural environment and  
42 on mucosal surfaces in mammals. It is also a bacterium of industrial importance as it is used for the  
43 production of numerous industrial chemicals. When this bacterium is cultured with glycerol as the main  
44 carbon source, 1,3-propanediol is the main metabolite and this process has a high conversion ratio and a  
45 high productivity (Hao et al. 2008). 1,3-Propanediol can be used to synthesize polytrimethylene  
46 terephthalate (PTT) and other industrial polyester fibers. This has resulted in the commercialization of  
47 1,3-propanediol production in China using *K. pneumoniae*. When *K. pneumoniae* is grown on other  
48 carbon sources such as glucose, the main metabolite is 2,3-butanediol (Chen et al. 2014). Acetoin is the  
49 metabolic precursor of 2,3-butanediol and high levels of acetoin have been produced in a strain (*K.*  
50 *pneumoniae*  $\Delta$ *budC*) in which the butanediol dehydrogenase gene has been inactivated (Wang et al. 2015).  
51 Acetoin is synthesized from  $\alpha$ -acetolactate, and this reaction is catalysed by  $\alpha$ -acetolactate decarboxylase.  
52 In another study, *K. pneumoniae*  $\Delta$ *budA*, the  $\alpha$ -acetolactate decarboxylase inactivated strain, produced  
53 2-ketoisovalerate and isobutanol at neutral pH conditions (Gu et al. 2017). The 2-ketoisovalerate and  
54 isobutanol synthesis pathway, the 2,3-butanediol synthesis pathway and the branched-chain amino acid  
55 synthesis pathway share some common steps in which pyruvate, a principal metabolite of the cell, is their  
56 main precursor compound. Two molecules of pyruvate condense to synthesize one molecule of  
57 acetolactate and this reaction is catalysed by isoenzymes of acetohydroxy acid synthase and  $\alpha$ -  
58 acetolactate synthase. 2,3-Dihydroxyisovalerate is synthesized from  $\alpha$ -acetolactate and this reaction is  
59 catalysed by the acetohydroxy acid isomeroreductase. 2,3-Dihydroxyisovalerate dehydrates to form 2-  
60 ketoisovalerate and the latter is further converted to valine and leucine (Fig. 1).  $\alpha$ -Acetolactate synthase  
61 and  $\alpha$ -acetolactate decarboxylase are encoded by the *budB* and *budA* genes, and they are located in the  
62 *bud* operon in *K. pneumoniae* (Blomqvist et al. 1993). *ilvBN*, *ilvGM*, *ilvIH* encode acetohydroxy acid  
63 synthase I, II and III. *ilvC*, *ilvD* and *ilvE* encoding acetohydroxy acid isomeroreductase, dihydroxy acid  
64 dehydratase and transaminase. *ilvGMED* and threonine dehydratase encoding gene *ilvA* forms a single  
65 operon, while *ilvBN*, *ilvIH*, and *ilvC* are independent operons in *Escherichia coli* and *K. pneumoniae*  
66 (Lawther et al. 1987, Gu et al. 2017).

67 2,3-Dihydroxyisovalerate is an intermediate of the valine and leucine synthesis pathway, however,  
68 there are no reports which confirm that this chemical can be produced naturally by microorganisms. An  
69 engineered *Saccharomyces cerevisiae* strain which was used for isobutanol production secreted 0.3 g/L  
70 of 2,3-dihydroxyisovalerate under microaerobic fermentation conditions (Generoso et al. 2017). Racemic

71 sodium salt of 2,3-dihydroxyisovalerate can be synthesized via a chemical approach (Cioffi et al. 1980).  
72 This was a laboratory method for 2,3-dihydroxyisovalerate preparation and the product was used to detect  
73 the activity of dihydroxyisovalerate dehydratase. It has been reported to be in the R-form in The Human  
74 Metabolome Database, and its main biological role being a nutrient, energy storage, energy source, and  
75 membrane stabilizer (<http://www.hmdb.ca/metabolites/HMDB0012141>). The specific chiral structure of  
76 (R)-2,3-dihydroxyisovalerate is highly attractive for modification which can lead to the formation of  
77 compounds of interest in the pharmaceutical industry. In particular, (R)-2,3-dihydroxyisovalerate is an  
78 intermediate of azinomycins synthesis which is known to exhibit potent antitumor activities (Bryant et  
79 al. 1998). Like lactic acid, 2,3-dihydroxyisovalerate has hydroxyl groups and a carboxyl group, which  
80 might allow possible applications in polymers synthesis. Currently, 2,3-dihydroxyisovalerate is not  
81 available in large quantity, especially the optical isomer, which limits its application. The biological route  
82 of 2,3-dihydroxyisovalerate production might provide an efficient way for the large scale production of  
83 this chemical, and enables its application in industry.

84 Here, we show for the first time 2,3-dihydroxyisovalerate synthesis by mutants of *K. pneumoniae* and  
85 partial optimization of the production process with regard to culture pH and agitation using a triple  
86 deletion mutant.

87

## 88 **Materials and methods**

### 89 **Strains, plasmids, and primers**

90 Bacterial strains and plasmids used in this study are listed in Table 1. Primers used for PCR are listed in  
91 Table 2.

### 92 **Construction of mutants of *K. pneumoniae***

93 For mutant constructions, *K. pneumoniae* and *E. coli* were grown in Luria–Bertani (LB) medium at 37 °C.  
94 The antibiotics used in the selective medium were ampicillin (50 µg/mL), kanamycin (50 µg/mL),  
95 apramycin (50 µg/mL), and streptomycin (25 µg/mL).

#### 96 *K. pneumoniae* $\Delta$ *ilvD* construction

97 Mutants were generated by following the methodology outlined by Wei et al (2012). The *ilvD* gene in  
98 *K. pneumoniae* and flanking sequences were amplified by PCR using the primer pair *ilvD*-s and *ilvD*-a.  
99 The PCR product was ligated into the pMD18-T vector to generate pMD18-T-*ilvD*. A linear DNA with  
100 39 and 40 nt homologous extensions flanking apramycin resistance gene *aac(3)IV* was amplified with  
101 plasmid pIJ773 as the template using the primer pair *ilvD*-FRT-s/*ilvD*-FRT-a. pMD18-T- $\Delta$ *ilvD* was

102 constructed by replacing *ilvD* in the plasmid pMD18-T-*ilvD* with the *aac(3)IV* cassette using the Red  
103 recombination system in *E. coli*.

104 pMD18-T- $\Delta$ *ilvD* was used as the template for PCR of a linear DNA containing the apramycin  
105 resistance gene *aac(3)IV* with 500 bp of *ilvD* homologous regions on both sides. The primer pair used  
106 was *ilvD*-a/*ilvD*-s. The linear DNA was transformed into *K. pneumoniae* CGMCC 1.6366, which already  
107 hosted the plasmid pDK6-red. Homologous recombination between the linear DNA and the chromosome  
108 was facilitated by Red recombinase and led to *ilvD* deletion in the genome of *K. pneumoniae* to obtain  
109 *K. pneumoniae*  $\Delta$ *ilvD*.

110 *K. pneumoniae*  $\Delta$ *budA*- $\Delta$ *ilvD* construction

111 *K. pneumoniae*  $\Delta$ *budA*- $\Delta$ *ilvD* was constructed following the same way of *K. pneumoniae*  $\Delta$ *ilvD*  
112 construction, with *K. pneumoniae*  $\Delta$ *budA* replacing wild-type *K. pneumoniae* as the target strain.

### 113 **2,3-Dihydroxyisovalerate purification and structure confirmation**

114 2,3-Dihydroxyisovalerate produced by *K. pneumoniae*  $\Delta$ *budA*- $\Delta$ *ldhA*- $\Delta$ *ilvD* was purified from the  
115 fermentation broth and its structure was confirmed by nuclear magnetic resonance (NMR) spectroscopic  
116 analysis. The cell-free broth of *K. pneumoniae*  $\Delta$ *budA*- $\Delta$ *ldhA*- $\Delta$ *ilvD* was discolored by activated carbon.  
117 The discolored broth was subsequently passed through an anion exchange (D311) column, which had  
118 been treated with 1 mol/L NaOH. The column was rinsed with water to neutral pH and gradient eluted  
119 with NH<sub>3</sub> solution (0-1 mol/L). Eluate fractions that contained the target compound were concentrated  
120 using a rotary evaporator. Crystals obtained were used for <sup>1</sup>H and <sup>13</sup>C nuclear magnetic resonance (NMR)  
121 spectroscopic analysis. A Bruker spectrometer was used and chemical shift values are reported in ppm  
122 ( $\delta$ ).

### 123 **Medium and culture conditions**

124 The fermentation medium contained 30-50 g/L glucose, 5 g/L yeast extract, 4 g/L corn steep liquor, 5 g/L  
125 (NH<sub>4</sub>)<sub>2</sub>SO<sub>4</sub>, 3 g/L sodium acetate, 0.4 g/L KCl, 0.1 g/L MgSO<sub>4</sub>, 0.02 g/L FeSO<sub>4</sub>, and 0.01 g/L MnSO<sub>4</sub>.  
126 Corn steep liquor free fermentation medium is a modified fermentation medium without corn steep liquor  
127 and the concentration of yeast extract is 1.5 g/L.

128 A single colony grown on plate was selected to inoculate into 50 ml of LB medium and grown for 12  
129 hours at a rotary shaker at 37°C and 200 rpm overnight. Then 1 ml of seed culture was inoculated into  
130 250 mL flasks containing 50 mL of fermentation medium for flask culture.

131 M9 minimal medium with different carbon sources (4 g/L) were used for carbon sources utilization  
132 experiments.

133 Fermentation parameters focusing on culture pH and agitation rate optimization experiments were  
134 performed in stirred tank bioreactors operated in batch mode. 50 ml of seed culture was inoculated into  
135 5-L bioreactor (BIOSTAT-A plus Sartorius) with a working volume of 3 L and the air flow rate of 2 L/min.  
136 The culture pH was automatically controlled by 2M NaOH solution.

137 Fed-batch cultures were performed at optimized conditions, with culture pH 6.5, culture temperature  
138 37°C and stirring rate of 400 rpm. When the glucose level in the broth decreased to 10 g/L, 200 mL of  
139 600 g/L glucose solution was added batch wise.

#### 140 **Analytical methods**

141 The biomass titer at set time intervals was determined by optical density (OD<sub>600</sub>) with a  
142 spectrophotometer. Cell dry weight (CDW) per liter of fermentation broth was calculated from OD values  
143 using the following formula:  $CDW (g/l) = 0.387 \times OD + 0.334$ .

144 Chemical compounds in the broth were quantified by a Shimadzu 20AVP high performance liquid  
145 chromatograph system (HPLC) equipped with a RID-20A refractive index detector and a SPD-M20A  
146 photodiode array detector. An Aminex HPX-87H column (300×7.8 mm) (Bio-Rad, USA) was used and  
147 the column temperature was set at 65 °C. The mobile phase was 0.025 mol/L H<sub>2</sub>SO<sub>4</sub> solution (pH 1.6)  
148 using a flow rate of 0.8 ml/min.

#### 149 **Carbon balance**

150 For carbon balance calculations, the elemental composition of *K. pneumoniae* was assumed to be  
151 CH<sub>1.73</sub>O<sub>0.43</sub>N<sub>0.24</sub> (Esener et al. 1982). Carbon recovery was calculated as percentage of total product  
152 carbon divided by total substrate carbon at the time point where the highest 2,3-dihydroxyisovalerate  
153 titer was reached.

154

#### 155 **Results**

##### 156 **2,3-Dihydroxyisovalerate purification and structure validation**

157 The *ilvD* gene which encodes dihydroxy acid dehydratase catalysed the reaction of 2-ketoisovalerate  
158 formation from 2,3-dihydroxyisovalerate. *K. pneumoniae*  $\Delta budA-\Delta ldhA-\Delta ilvD$  was constructed in our  
159 previous research of 2-ketoisovalerate and isobutanol production, and 2-ketoisovalerate and isobutanol  
160 synthesis was blocked in this strain (Gu et al. 2017). We suspected 2,3-dihydroxyisovalerate might have  
161 accumulated in the broth of this strain during fermentation and the potential fraction was purified from  
162 the broth. The fermentation broth of *K. pneumoniae*  $\Delta budA-\Delta ldhA-\Delta ilvD$  contained a range of organic  
163 acids such as succinic acid and acetic acid. The potential fraction in the fermentation broth was purified

164 by ion-exchange chromatography. <sup>1</sup>H and <sup>13</sup>C NMR spectral data of the sample are given in Table 3.

165 The <sup>1</sup>H NMR data correlate with the report of the chemical synthesized racemic sodium salt of 2,3-  
166 dihydroxyisovalerate (Cioffi et al. 1980) and reports from urine samples from patients (Holmes et al.  
167 1997). <sup>13</sup>C NMR data of 2,3-dihydroxyisovalerate were not found in other reports. The predicted <sup>13</sup>C  
168 NMR shift by ChemDraw was 173.2, 86.3, 70.9, and 23.1 for C1, C2, C3, and C4, C5. Thus, the structure  
169 of 2,3-dihydroxyisovalerate produced by *K. pneumoniae*  $\Delta budA-\Delta ldhA-\Delta ilvD$  was confirmed.

### 170 **2,3-Dihydroxyisovalerate production by mutants of *K. pneumoniae***

171 To investigate the mechanism of 2,3-dihydroxyisovalerate accumulation, *K. pneumoniae*  $\Delta ilvD$  and *K.*  
172 *pneumoniae*  $\Delta budA-\Delta ilvD$  were constructed. These two strains and the wild-type *K. pneumoniae*, *K.*  
173 *pneumoniae*  $\Delta budA$  and *K. pneumoniae*  $\Delta budA-\Delta ldhA-\Delta ilvD$  were cultured in shake flasks with the corn  
174 steep liquor free fermentation medium and the results are shown in Fig. 2.

175 The cell growth of wild-type strain, *K. pneumoniae*  $\Delta budA$  and *K. pneumoniae*  $\Delta ilvD$  were very similar  
176 during the first 6 hours of cultivation. After that time, the wild-type strain continued to grow at a fast rate  
177 until all the glucose was consumed reaching a final cell density of  $8.6 \pm 0.9$  OD units after 10 hours. By  
178 contrast, growth of the *K. pneumoniae*  $\Delta ilvD$  mutant ended after about 8 hours reaching a final cell  
179 density of  $3.6 \pm 0.2$  OD units. After that point, the cell density decreased slightly though the cells still  
180 consumed glucose until the end of the cultivation. The *K. pneumoniae*  $\Delta budA$  mutant reached a cell  
181 density of  $5.8 \pm 0.3$  OD units after 12 hours when most of the glucose was consumed. From that point the  
182 cell density decreased until it reached a final value of about  $4.1 \pm 0.01$  OD units after 20 hours. In contrast  
183 to the single mutants, growth of the *K. pneumoniae*  $\Delta budA-\Delta ilvD$  and *K. pneumoniae*  $\Delta budA-\Delta ldhA-$   
184  $\Delta ilvD$  mutants was very weak, and the final cell densities were only  $1.5 \pm 0.2$  OD and  $0.5 \pm 0.1$  OD units,  
185 respectively. Despite, the slow growth both mutants consumed most of the glucose by end of the  
186 cultivation. The glucose consumption of all strains coincided with cell growth and was similar for the  
187 first 6 hours (Fig. 2A). After the initial growth period clear differences in glucose utilization could be  
188 seen with the wild-type strain exhibiting the highest rate of consumption followed by *K. pneumoniae*  
189  $\Delta budA$ , *K. pneumoniae*  $\Delta ilvD$ , *K. pneumoniae*  $\Delta budA-\Delta ilvD$ , and *K. pneumoniae*  $\Delta budA-\Delta ldhA-\Delta ilvD$   
190 that had the lowest glucose consumption rate. 2,3-Butanediol was the main metabolite of the wild-type  
191 strain yielding 5.1 g/L. Yet although the 2,3-butanediol production was lower for the *K. pneumoniae*  
192  $\Delta ilvD$  mutant with a titer of 1.3 g/L, it was still the main metabolite of this strain. Acetic acid was  
193 produced by all strains and *K. pneumoniae*  $\Delta budA$  had the highest titer of 2.5 g/L after 15 hours. The  
194 others mutants reached similar levels of about 2 g/L at the end of the cultivation. Lactic acid was the

195 major product of the *K. pneumoniae*  $\Delta budA$  mutant with levels increasing to 2.2 g/L after 15 hours.  
196 However, only 0.3 g/L of lactic acid was produced by *K. pneumoniae*  $\Delta budA-\Delta ilvD$  and no lactic acid  
197 was detected in the broth of *K. pneumoniae*  $\Delta budA-\Delta ldhA-\Delta ilvD$ . In this mutant, the lactic acid synthesis  
198 pathway was blocked by disruption of the *ldhA* gene, which encodes a lactate dehydrogenase. As  
199 expected no 2,3-Butanediol was synthesized by *K. pneumoniae*  $\Delta budA-\Delta ilvD$  because the 2,3-butanediol  
200 synthesis pathway was blocked by disruption of *budA*. 2,3-dihydroxyisovalerate produced by this double  
201 deletion mutant was 3.3 g/L and the titer was further increased to 3.7 g/L by *K. pneumoniae*  $\Delta budA-$   
202  $\Delta ldhA-\Delta ilvD$  at the end of the cultivation. These titers were much greater than the 0.2 g/L produced by  
203 *K. pneumoniae*  $\Delta ilvD$ . *K. pneumoniae*  $\Delta budA$  produced 1.6 g/L of 2,3-dihydroxyisovalerate after 17  
204 hours of cultivation, which was comparable to that produced by *K. pneumoniae*  $\Delta budA-\Delta ilvD$  at the same  
205 time. However, after the glucose was exhausted, the accumulated 2,3-dihydroxyisovalerate was reused  
206 by the *K. pneumoniae*  $\Delta budA$  cells. Due to the high production of 2,3-dihydroxyisovalerate coupled with  
207 the lowest by-product formation only *K. pneumoniae*  $\Delta budA-\Delta ldhA-\Delta ilvD$  was further characterized.

### 208 **2,3-Dihydroxyisovalerate production using different carbon sources**

209 *K. pneumoniae* is a bacterium that is capable of utilizing a range of different carbon sources such as  
210 glucose, xylose and glycerol for 2,3-butanediol and other chemicals production. Thus these were used as  
211 the sole carbon source in minimal medium to evaluate their utilization for the 2,3-dihydroxyisovalerate  
212 production by *K. pneumoniae*  $\Delta budA-\Delta ldhA-\Delta ilvD$  (Fig. 3).

213 After 90 hours of cultivation, the cells consumed about 3 g/L of these three carbon sources considering  
214 the slightly different starting concentrations. Final 2,3-Dihydroxyisovalerate titers of 1.0, 1.0, and 0.7  
215 g/L using glucose, xylose or glycerol as carbon sources, respectively were obtained. In addition, 0.025  
216 g/L of 1,3-propanediol was produced with glycerol as the carbon source.

217 Cell growth in minimal medium with either glucose, xylose, or glycerol as the sole carbon source was  
218 very weak, with all cell densities obtained lower than 0.3 OD units (data not shown). The likely reason  
219 for the poor growth was the lack of branched-chain amino acids in the medium. To further investigate  
220 carbon source utilization, a complex nutrient-rich medium containing corn steep liquor was used. *K.*  
221 *pneumoniae*  $\Delta budA-\Delta ldhA-\Delta ilvD$  was cultured in this fermentation medium with either glucose, xylose  
222 or glycerol as the main carbon source, and results are shown in Fig. 4.

223 The cell growth was similar for the first 10 hours of cultivation on all three carbon sources tested.  
224 Cells on xylose continued to grow at a fast rate reaching a final OD of 4.3 after 23 hours of cultivation,  
225 while consuming about 68% (23 g/L) of the initial xylose concentration. Cells on glucose grow slightly



226 slower reaching an OD of 2.7 after 23 hours at which point all the glucose supplied was consumed.  
227 Whereas the cells grown on glycerol only reached an OD of 1.6 after 17 hours of cultivation when the  
228 glycerol ran out, and 9.9 g/L of 1,3-propanediol was produced. The 2,3-dihydroxyisovalerate synthesis  
229 was at a similar rate using these carbon sources leading to 7.4 g/L, 7.0 g/L, and 4.6 g/L of 2,3-  
230 dihydroxyisovalerate being produced, with the conversion ratio of 0.25, 0.32, and 0.16 (g/g) using  
231 glucose, xylose and glycerol, respectively. Thus both glucose and xylose are suitable carbon sources for  
232 2,3-dihydroxyisovalerate production. Considering the lower cost of glucose compared to xylose, glucose  
233 was selected as carbon source for further studies.

#### 234 **Fermentation parameters optimization**

235 *K. pneumoniae* has been used as producer for many chemicals production requiring different process  
236 conditions with regard to oxygen levels and culture pH. Here culture pH and agitation rates for 2,3-  
237 dihydroxyisovalerate production were optimized separately.

238 Culture pH optimization.

239 Based on the shake flasks data *K. pneumoniae*  $\Delta budA-\Delta ldhA-\Delta ilvD$  was cultured in 5 L bioreactors with  
240 fermentation medium using glucose as the main carbon source, the stirring rate was keep at 300 rpm and  
241 the air flow rate was set at 2L/min, where the culture pH was controlled at 6.0, 6.5, 7.0, 7.5, and 8.0.  
242 Fermentation results are presented in Fig. 5.

243 When cultured at pH 6.0, the cell growth and glucose consumption rates were the slowest amongst all  
244 the experimental pH ranges investigated. However, 2,3-dihydroxyisovalerate production was the highest  
245 at this condition, obtaining a titer of 15.9 g/L after 27 hours. The cell growth, glucose consumption rate,  
246 and 2,3-dihydroxyisovalerate production at the culture of pH 6.5 followed a similar pattern of the cells  
247 cultured at pH 6.0, with 14.7 g/L of 2,3-dihydroxyisovalerate being produced after 18 hours. Cell growth  
248 rates and glucose consumption rates at the culture pH 7.0-8.0 were similar. Based on these results it  
249 appears that 2,3-dihydroxyisovalerate production was inversely related to the culture pH. The 2,3-  
250 dihydroxyisovalerate level decreased to 8.2 g/L at the condition of culture pH 8.0.

251 The organic acid by-products generated by the cells, which included succinic acid, acetic acid, and  
252 formic acid, all appeared to have a positive correlation with the culture pH. The higher the pH culture,  
253 the more organic acids were produced. 3.5 g/L of succinic acid, 8.9 g/L of acetic acid, and 9.5 g/L of  
254 formic acid were produced at the culture pH of 8.0. By contrast, much less organic acids were produced  
255 by the cells grown at pH 6.0 i.e. 1.8 g/L, 0.4 g/L, and 0.5 g/L, respectively. Ethanol was another by-  
256 product of these cells, where a maximum ethanol titer of about 4.5 g/L was produced from the 6.5-7.5

257 pH cultures, whilst the lowest titers of about 2.5 g/L were obtained from cells grown at 6.0 and 8.0. Based  
258 on the production of metabolites and biomass, the carbon balance calculated for culture under pH 6.0,  
259 pH 6.5, pH 7.0, pH 7.5, and pH 8.0 are 73%, 75%, 81%, 81% and 78%, respectively. Thus, most of the  
260 carbon from glucose consumed is accounted for. The missing carbon is likely to be CO<sub>2</sub> generated from  
261 TCA cycle and decarboxylation reactions and additionally a small amount of other chemicals that were  
262 undetectable with the analysis method used here may have been formed.

263 It can be concluded from Fig. 5, that acidic conditions favor 2,3-dihydroxyisovalerate synthesis, but  
264 extreme acidic conditions inhibited the cell growth and affected the productivity. Considering both the  
265 substrate conversion ratio and the productivity, pH 6.5 was selected as the optimal culture pH.

266 Optimization of agitation rate

267 *K. pneumoniae*  $\Delta budA-\Delta ldhA-\Delta ilvD$  was cultured in 5L bioreactors with fermentation medium controlled  
268 at pH 7.0, and the air flow rate was set at 2L/min. The stirring rate of the bioreactor was set at 200, 300,  
269 400, 600, and 800 rpm to obtain different aerobic conditions. Fermentation results are presented in Fig.  
270 6.

271 Cell growth and glucose consumption appeared not to differ in these conditions. However, the amount  
272 of 2,3-dihydroxyisovalerate produced by these cultures were distinctly different. The highest 2,3-  
273 dihydroxyisovalerate titer of 18.7 g/L was produced at the stirring rate of 400 rpm, followed by stirring  
274 rate of 200 and 300 rpm generating 14.7 and 14.0 g/L of 2,3-dihydroxyisovalerate, respectively. Both  
275 growth and product formation were almost identical despite a 10% lower initial glucose concentration  
276 used in the cultivation operated at 300 rpm. Cultures grown with stirring rates of 600 and 800 rpm had  
277 the lowest 2,3-dihydroxyisovalerate production, with final titers of 10.5 and 9.3 g/L, respectively.

278 The amount of succinic acid, formic acid, and ethanol produced appears to have an inverse correlation  
279 with agitation rate. Using a stirring rate of 200 rpm, succinic acid, formic acid, and ethanol production  
280 was 2.4 g/L, 8.3 g/L, and 5.2 g/L, respectively. While using a stirring rate 600 and 800 rpm, these  
281 metabolites were not detected. However, 9.7 g/L and 8.7 g/L of acetic acid were produced at high  
282 agitation rates of 600 and 800 rpm, respectively. The carbon balance calculated for stirring rate of 200  
283 rpm, 300 rpm, 400 rpm, 600 rpm and 800 rpm are 77%, 75%, 68%, 53% and 48%, respectively. The  
284 lower carbon recoveries at stirring rates of 600 and 800 rpm are likely due to increased TCA cycle activity  
285 under fully aerobic conditions generating more CO<sub>2</sub>.

286 Looking at the data there is a very sharp change in metabolite production between low (200 - 400 rpm)  
287 vs. high (600-800 rpm) agitation conditions, especially for succinic acid, ethanol and formic acid

288 production. The increase of stirring rate from 400 rpm to 600 rpm can be considered as the change from  
289 medium to fully aerobic condition. The results suggests that the medium level of agitation (400 rpm)  
290 favors 2,3-dihydroxyisovalerate synthesis.

### 291 **Fed batch fermentation**

292 After the culture pH and agitation rate were optimized individually, fed batch fermentations were  
293 conducted to obtain a high final product level. Fermentation results are presented in Fig. 7.

294 In fed batch fermentation, cells exponentially grew for the first 10 hours, which resulted in a rapid  
295 depletion of glucose. Cells then reached a stationary phase and the glucose concentration in the broth  
296 dropped to 10 g/L after 12 hours. At this point a pulse of highly concentrated glucose solution was added  
297 and the glucose concentration increased to 45 g/L. After 24 hours, another glucose pulse feeding was  
298 performed. However at this stage, the cell density started to decrease, yet 2,3-dihydroxyisovalerate  
299 accumulation in the broth continued at a slow rate. Based on the production of 2,3-dihydroxyisovalerate  
300 (Fig. 7C), the process can be divided into three phases. From 0 to 6 hours there was a slow initial  
301 production phase coinciding with onset of cell growth. Once the cells entered the exponential growth  
302 phase the productivity increased rapidly with an average value of 1.85 g/L h between 6-21 hours. After  
303 the cells entered stationary phase the productivity in the third phase (21 - 45 hours) decreased to about  
304 0.28 g/L h. Overall, 36.5 g/L of 2,3-dihydroxyisovalerate was produced after 45 hours of cultivation. The  
305 maximum theoretical yield of 2,3-dihydroxyisovalerate synthesis from glucose is 1.0 mol/mol. The  
306 conversion ratio of 2,3-dihydroxyisovalerate from glucose was 0.58 mol/mol over the first 21 hours, and  
307 the conversion ratio of the whole process was 0.49 mol/mol. In agreement with the batch fermentation  
308 under the same conditions the main by-product was acetic acid, achieving a titer of 14.3 g/L; whereas  
309 the succinic acid formed was fully consumed by end of the process, and formic acid and ethanol were  
310 present at low concentrations, with 1.2 g/L and 0.3 g/L, respectively. The carbon recovery calculated was  
311 76% for the whole process. This value is in agreement with the carbon recovery of the batch fermentation  
312 performed under these conditions.

### 313 **Discussion**

#### 314 **2,3-Dihydroxyisovalerate and branched-chain amino acid synthesis pathway**

315 Branched-chain amino acids, including valine, leucine and isoleucine, are major building blocks of the  
316 cell. Their synthesis in the cell is strictly controlled by feedback inhibition and repression. The activity  
317 of *IlvBN* and *IlvIH* was inhibited by valine (Lawther et al. 1981). The *ilvBN* and *ilvGM* operons are  
318 repressed in cells grown in media containing excess branched-chain amino acids. The *ilvIH* operon is

319 repressed in cells growing in a medium containing leucine (Platko et al. 1990). Thus, synthesis of these  
320 amino acids will not exceed cell demand. In this study, the disruption of *ilvD* blocked the branched-chain  
321 amino acid pathway and induced 2,3-dihydroxyisovalerate accumulation in the broth (Fig. 2). The  
322 accumulation of intermediates by blocking metabolic pathways is common in bacteria. In our previous  
323 research acetoin accumulated in the broth of *K. pneumoniae*- $\Delta$ budC, in which butanediol dehydrogenase  
324 was inactivated (Wang et al. 2015). Furthermore, gluconic acid accumulated in the broth of *K.*  
325 *pneumoniae*- $\Delta$ gad, in which gluconate dehydrogenase was inactivated (Wang et al. 2016). The 2,3-  
326 dihydroxyisovalerate accumulated by *K. pneumoniae*- $\Delta$ ilvD was at a low concentration which suggested  
327 that the metabolic flux of the branched-chain amino acid synthesis pathway was not strong in *K.*  
328 *pneumoniae*. The stereochemistry of valine synthesis pathway is known. (S)-acetolactate is the substrate  
329 of acetohydroxy acid isomeroeductase and (R)-2,3-dihydroxyisovalerate is the product (Hill and Yan.  
330 1971; Chunduru et al. 1989; Dumas et al. 2001). Thus, 2,3-dihydroxyisovalerate obtained here was  
331 enantiomerically in R-form. The structure of this chemical was confirmed by NMR, and this optical  
332 isomer has important economic value.

### 333 **Disruption of *budA* resulted in 2,3-dihydroxyisovalerate accumulation**

334 2,3-Butanediol is the main metabolite of *K. pneumoniae*, suggesting that the carbon flux through the 2,3-  
335 butanediol synthesis pathway was very high. 2,3-Butanediol is less toxic than organic acids and 2,3-  
336 butanediol synthesized from different carbon sources prevents lethal acidification which is typically  
337 caused by the production of organic acids (Van Houdt et al. 2007). The first step of the 2,3-butanediol  
338 synthesis pathway shares the same step of the branched-chain amino acid synthesis, although the  
339 enzymes catalysing this step are different.  $\alpha$ -Acetolactate synthase encoded by *budB* is present in the 2,3-  
340 butanediol synthesis pathway, and acetohydroxy acid synthase I, II, and III encoded by *ilvBN*, *ilvGM*,  
341 *ilvIH* are used in the branched-chain amino acid synthesis pathway. Among these isoenzymes,  $\alpha$ -  
342 acetolactate synthase is mainly responsible for  $\alpha$ -acetolactate formation in *K. pneumoniae*. Branched-  
343 chain amino acid synthesis consumes a small percentage of  $\alpha$ -acetolactate, and most  $\alpha$ -acetolactate is  
344 used for 2,3-butanediol synthesis in *K. pneumoniae* (Gu et al. 2017). The 2,3-butanediol synthesis  
345 pathway and the branched-chain amino acid synthesis pathway are existing in parallel and do not interfere  
346 with each other in the wild-type *K. pneumoniae*. The 2,3-butanediol synthesis pathway was blocked by  
347 the disruption of *budA*, however, the activity of  $\alpha$ -acetolactate synthase was not affected. Thus,  $\alpha$ -  
348 acetolactate synthesized in the cell flowed into the valine and leucine synthesis pathway and resulted in  
349 2,3-dihydroxyisovalerate accumulation (Fig 1). This is in agreement with previously published research

350 on 2-ketoisovalerate accumulation by *K. pneumoniae*  $\Delta budA$  (Gu et al. 2017). The blocking of 2,3-  
351 butanediol synthesis pathway is critical for 2,3-dihydroxyisovalerate accumulation, as *K. pneumoniae*  
352  $\Delta budA$  accumulated 1.6 g/L of 2,3-dihydroxyisovalerate, which is 9 times higher than that accumulated  
353 by *K. pneumoniae*  $\Delta ilvD$  (Fig. 2). 0.7 g/L of 2,3-butanediol was produced by *K. pneumoniae*  $\Delta budA$  after  
354 23 hours of cultivation (Fig. 2). The likely reason is that  $\alpha$ -acetolactate is unstable and can be converted  
355 to diacetyl by nonenzymatic oxidation, and diacetyl formed can be converted to acetoin and further to  
356 2,3-butanediol (Xiao and Xu. 2007). There are numerous reports about 2,3-butanediol production by *K.*  
357 *pneumoniae*, and some strains have a very high 2,3-butanediol producing ability (Ma et al. 2009). These  
358 strains might be better chassis cells for 2,3-dihydroxyisovalerate producing strain construction.

### 359 **Disruption of *ilvD* prevented conversion of 2,3-dihydroxyisovalerate**

360 2-Ketoisovalerate is an intermediate product of the valine and leucine synthesis pathway. Disruption of  
361 the *ilvD* gene will block 2-ketoisovalerate synthesis from 2,3-dihydroxyisovalerate and will result in  
362 amino acid auxotrophy. Beside branched-chain amino acids, pantothenic acid is also synthesized from 2-  
363 ketoisovalerate, and this strain was also auxotrophic for pantothenic acid. When cultured in the corn steep  
364 liquor free fermentation medium, the available nutrition limited the growth of *K. pneumoniae*  $\Delta ilvD$  and  
365 affected the 2,3-butanediol synthesis (Fig 2). When cultured in fermentation medium, cell growth and  
366 2,3-butanediol production were similar between *K. pneumoniae*  $\Delta ilvD$  and the wild-type strain (data not  
367 shown). As 2,3-dihydroxyisovalerate can further be converted to 2-ketoisovalerate, the accumulated 2,3-  
368 dihydroxyisovalerate can be reused by the *K. pneumoniae*  $\Delta budA$  cells. Combined disruption of *ilvD* and  
369 *budA* resulted in a high and stable 2,3-dihydroxyisovalerate production.

### 370 **Blocking of lactic acid synthesis enhanced 2,3-dihydroxyisovalerate production**

371 Lactic acid is synthesized from pyruvate and lactic acid production bypasses other pathways, which use  
372 pyruvate as the initial substrate. Conversion of pyruvate to lactic acid consumes one molecule of NADH,  
373 and the saved NADH might affect other chemicals synthesis. As such, the final level of 1,3-propanediol  
374 distinctly increased by *K. pneumoniae*  $\Delta ldhA$  (Xu et al. 2009). When using glucose as the sole carbon  
375 source, the amount of lactic acid produced by wild-type *K. pneumoniae* was not particularly high, and  
376 the knock-out of *ldhA* had little influence on 2,3-butanediol production (Guo et al. 2014). However, when  
377 the 2,3-butanediol synthesis pathway was blocked, lactic acid synthesis increased to a high level (Fig.2).  
378 This validated our previous research on 2-ketoisovalerate and isobutanol production by *K. pneumoniae*  
379 (Gu et al. 2017). Beside lactic acid, removal of other by-products such as acetic acid and ethanol  
380 increased 2,3-butanediol synthesis by *K. pneumoniae* (Guo et al. 2014; Rathanasingh et al. 2016). These

381 metabolic engineering strategies might be adopted to improve 2,3-dihydroxyisovalerate synthesis.

382 **Acidic and medium aerobic conditions favor 2,3-dihydroxyisovalerate synthesis**

383 Culture parameters of 2,3-dihydroxyisovalerate production such as culture temperature, air flow rate and  
384 the content of the medium were based on those used for 2,3-butanediol and 2-ketoisovalerate production  
385 in our previous research (Gu et al. 2017). Thus only agitation rate and culture pH were optimized here.  
386 The optimal culture pH for 1,3-propanediol production by *K. pneumoniae* was in neutral pH conditions  
387 (Hao et al. 2008), which is in agreement with the optimal pH for *K. pneumoniae* cell growth (Sun et al.  
388 2014). However, in the pH range from 5.5-6.5, 2,3-butanediol production by *K. pneumoniae* had the  
389 highest conversion ratio (Zeng et al. 1990), which was similar for acetoin production (Wang et al. 2015).  
390 Similarly, when *K. pneumoniae* was grown with glycerol as the carbon source it was shown that lower  
391 pH favor 2,3-butanediol formation and inhibit acetic acid synthesis (Biebl et al. 1998). The 2,3-  
392 butanediol production by an *Enterobacter cloacae* strain also showed an optimal culture pH of 6.5 (Priya  
393 et al. 2016). The transcription of the *bud* operon of *Klebsiella terrigena* is induced at oxygen-limited  
394 acidic conditions, 2,3-butanediol production prevents acetate overproduction and subsequent  
395 intracellular acidification (Blomqvist et al. 1993). 2,3-Dihydroxyisovalerate synthesis shares the first  
396 step of 2,3-butanediol synthesis pathway. Thus the optimal pH for 2,3-dihydroxyisovalerate production  
397 coincided with that of the 2,3-butanediol and acetoin production. In this study, a higher pH culture  
398 favored synthesis of succinic acid, acetic acid, and formic acid by-products. Formic acid was formed  
399 from pyruvate and catalysed by pyruvate formate-lyase. Higher formic acid levels suggested that more  
400 pyruvate was converted to acetyl-CoA (Zhou et al. 2017). Acetyl-CoA is a central metabolite and used  
401 for synthesis of many building blocks or catabolism through the TCA cycle. Acetyl-CoA can be converted  
402 to acetaldehyde and further converted to acetic acid. This resulted in higher acetic acid levels produced  
403 at higher culture pH values in this study. Succinic acid is an intermediate metabolite of the TCA cycle.  
404 Higher succinic acid production at higher culture pH might be the result of more acetyl-CoA flowing into  
405 the TCA cycle.

406 Medium agitation rates corresponding to medium aerobic conditions favor 2,3-dihydroxyisovalerate  
407 production, which is in agreement with 2-ketoisovalerate production by *K. pneumoniae* (Gu et al. 2017).  
408 In 2,3-butanediol production by *K. pneumoniae*, high oxygen levels can completely hinder the butanediol  
409 formation (Silveira et al. 1993). It has been reported that under high aerobic conditions  $\alpha$ -acetolactate  
410 synthase was rapidly and irreversibly inactivated in *K. pneumoniae* and prevented 2,3-butanediol  
411 synthesis (Kosaric et al. 1992). This is different from valine production by *Brevibacterium flavum* (Huang

412 et al. 2018) or *Corynebacterium glutamicum* (Blombach et al. 2007), which are all highly aerobic  
413 processes. The *bud* operon is induced by oxygen-limited conditions (Blomqvist et al. 1993). While, there  
414 has been no report about the effect of oxygen on *ilvC* expression, *ilvC* is induced by acetohydroxybutyrate  
415 or acetolactate in *E. coli* (Arfin et al. 1969). The medium aerobic condition favoring high 2,3-  
416 dihydroxyisovalerate production may be related to NADH regeneration to maintain the glycolytic flux.  
417 There are some reports about succinic acid and ethanol production by *K. pneumoniae*, and these studies  
418 were all performed under anaerobic or microaerobic conditions (Chandresh et al. 2006; Oh et al. 2013).  
419 This is agreement with our results of succinic acid and ethanol production that were inhibited under high  
420 aerobic conditions.

421 This is the first report to propose a biological route for the production of 2,3-dihydroxyisovalerate by  
422 the bacterium *K. pneumoniae*. A final titer of 36.5 g/L of 2,3-dihydroxyisovalerate were achieved in 45  
423 hours of fed-batch fermentation equating to a conversion ratio of 0.49 mol/mol glucose. If the process  
424 would have been terminated after 21 hours, a conversion ratio of 0.58 mol/mol glucose and an overall  
425 productivity of about 1.4 g/L h, could have been obtained with a final titer of about 30 g/L. The  
426 conversion ratio and final titer are approaching that of valine production by *B. flavum* (0.6 mol/mol, 70  
427 g/L) and *C. glutamicum* (0.6 mol/mol and 23 g/L) (Huang et al. 2018, Blombach et al. 2007). Thus this  
428 process has the potential to be industrialized for 2,3-dihydroxyisovalerate production assuming a similar  
429 product price to that of valine.

430

431 **Conflict of Interest:** Authors declare that they have no conflict of interest.

432

433 **Acknowledgements:** This study was funded by National Key R&D Program of China (Grant No.  
434 2017YFE0112700), Royal Society-Newton Advanced Fellowship (Grant No. NAF\R2\180721), Natural  
435 Science Foundation of Shanghai (Grant No. 19ZR1463600) and National Natural Science Foundation of  
436 China (Grant No. 21576279). FB would like to thank the Chinese Academy of Sciences for the award of  
437 a President's International Fellowship Initiative (Grant No. 2019VCB0007).

438

439 **Compliance with Ethical Standards:** This article does not contain any studies with human participants  
440 or animals performed by any of the authors.

441

#### 442 **References**

443 Arfin SM, Ratzkin B, Umbarger HE (1969) The metabolism of valine and isoleucine in *Escherichia coli*.

444 XVII. The role of induction in the derepression of acetohydroxy acid isomeroreductase.  
445 Biochem Biophys Res Commun 37: 902-908

446 Biebl H, Zeng AP, Menzel K, Deckwer WD (1998) Fermentation of glycerol to 1,3-propanediol and 2,3-  
447 butanediol by *Klebsiella pneumoniae*. Appl Microbiol Biotechnol 50:24–9

448 Blombach B, Schreiner ME, Holátko J, Bartek T, Oldiges M, Eikmanns BJ (2007) L-valine production  
449 with pyruvate dehydrogenase complex-deficient *Corynebacterium glutamicum*. Appl Environ  
450 Microbiol 73(7):2079-2084

451 Blomqvist K, Nikkola M, Lehtovaara P, Suihko M, Airaksinen U, Stråby K, Knowles J, Penttilä M (1993)  
452 Characterization of the genes of the 2, 3-butanediol operons from *Klebsiella terrigena* and  
453 *Enterobacter aerogenes*. J Bacteriol 175(5):1392-1404

454 Bryant H, Dardonville C, Hodgkinson T, Hursthouse M, Malik KáA (1998) Asymmetric synthesis of the  
455 left hand portion of the azinomycins. J Chem Soc Perk T 1(7):1249-1256

456 Chandresh T, Bhosale S, Ranade D (2006) Formation of Succinic Acid by *Klebsiella pneumoniae* MCM  
457 B-325 Under Aerobic and Anaerobic Conditions. J Microbiol Biotechnol 16(6): 870–879

458 Chen C, Wei D, Shi J, Wang M, Hao J (2014) Mechanism of 2, 3-butanediol stereoisomer formation in  
459 *Klebsiella pneumoniae*. Appl Microbiol Biotechnol 98(10):4603-4613

460 Chunduru SK, Mrachko GT, Calvo KC (1989) Mechanism of ketol acid reductoisomerase - Steady-state  
461 analysis and metal ion requirement. Biochem 28(2):486-493

462 Cioffi EA, Shaw KJ, Bailey WF, Berg CM (1980) Improved synthesis of the sodium salt of DL- $\alpha$ ,  $\beta$ -  
463 dihydroxyisovaleric acid. Anal Biochem 104(2):485-488

464 Dumas R, Biou V, Halgand F, Douce R, Duggleby RG (2001) Enzymology, Structure, and Dynamics of  
465 Acetohydroxy Acid Isomeroreductase. Acc Chem Res 34(5):399-408

466 Esener AA, Roels JA, Kossen NWF (1982) Dependence of elemental composition of *K. pneumoniae* on  
467 the steady-state specific growth rate. Biotechnol Bioeng 24: 1445-1449

468 Generoso WC, Brinek M, Dietz H, Oreb M, Boles E (2017) Secretion of 2, 3-dihydroxyisovalerate as a  
469 limiting factor for isobutanol production in *Saccharomyces cerevisiae*. FEMS Yeast Res 17(3)

470 Gu J, Zhou J, Zhang Z, Kim CH, Jiang B, Shi J, Hao J (2017) Isobutanol and 2-ketoisovalerate production  
471 by *Klebsiella pneumoniae* via a native pathway. Metab Eng 43:71-84

472 Guo X, Cao C, Wang Y, Li C, Wu M, Chen Y, Zhang C, Pei H, Xiao D (2014) Effect of the inactivation  
473 of lactate dehydrogenase, ethanol dehydrogenase, and phosphotransacetylase on 2, 3-butanediol  
474 production in *Klebsiella pneumoniae* strain. Biotechnol Biofuels 7(1):44

475 Gust B, Challis GL, Fowler K, Kieser T, Chater KF (2003) PCR-targeted *Streptomyces* gene replacement  
476 identifies a protein domain needed for biosynthesis of the sesquiterpene soil odor geosmin. P  
477 Natl Acad Sci USA 100(4):1541-1546

478 Hao J, Lin R, Zheng Z, Liu H, Liu D (2008) Isolation and characterization of microorganisms able to  
479 produce 1, 3-propanediol under aerobic conditions. World J Microbiol Biotechnol 24(9):1731-  
480 1740

481 Hill RK, Yan S-J (1971) Stereochemistry of valine and isoleucine biosynthesis II. Absolute configuration  
482 of (-)- $\alpha$ , $\beta$ -dihydroxyisovaleric acid and (-)- $\alpha$ , $\beta$ -dihydroxy- $\beta$ -methylvaleric acid. Bioorganic  
483 Chem 1(4):446-456

484 Holmes E, Foxall PJ, Spraul M, Farrant RD, Nicholson JK, Lindon JC (1997) 750 MHz 1H NMR  
485 spectroscopy characterisation of the complex metabolic pattern of urine from patients with  
486 inborn errors of metabolism: 2-hydroxyglutaric aciduria and maple syrup urine disease. J Pharm  
487 Biomed Anal 15(11):1647-1659



488 Huang Q-G, Zeng B-D, Liang L, Wu S-G, Huang J-Z (2018) Genome shuffling and high-throughput  
489 screening of *Brevibacterium flavum* MDV1 for enhanced L-valine production. *World J*  
490 *Microbiol Biotechnol* 34(8):121

491 Kosaric N, Magee R, Blaszczyk R (1992) Redox potential measurement for monitoring glucose and  
492 xylose conversion by *K. pneumoniae*. *Chem Biochem Eng Q* 6:145–52

493 Lawther RP, Calhoun DH, Adams CW, Hauser CA, Gray J, Hatfield GW (1981) Molecular basis of valine  
494 resistance in *Escherichia coli* K-12. *P Natl Acad Sci USA* 78(2):922-925

495 Lawther RP, Wek RC, Lopes JM, Perira R, Taillon BE, Wesley G (1987) The complete nucleotide  
496 sequence of the ilvGMEDA operon of *Escherichia coli* K-12. *Nucleic Acids Res* 15(5):2137-  
497 2155

498 Ma C, Wang A, Qin J, Li L, Ai X, Jiang T, Tang H, Xu P (2009) Enhanced 2,3-butanediol production by  
499 *Klebsiella pneumoniae* SDM. *Appl Microbiol Biotechnol* 82:49-57

500 Oh BR, Hong WK, Heo SY, Joe M, Seo JW, Kim CH (2013) The role of aldehyde/alcohol dehydrogenase  
501 (AdhE) in ethanol production from glycerol by *Klebsiella pneumoniae*. *J Ind Microbiol*  
502 *Biotechnol* 40:227–233

503 Platko JV, Willins DA, Calvo JM (1990) The ilvIH operon of  
504 *Escherichia coli* is positively regulated. *J Bacteriol* 172(8):4563-4570

505 Priya A, Dureja P, Talukdar P, Rath R, Lal B, Sarma PM (2016) Microbial production of 2,3-butanediol  
506 through a two-stage pH and agitation strategy in 150 l bioreactor. *Biochem Eng J* 105: 159-167

507 Rathnasingh C, Park J M, Kim D, Song H, Chang YK (2016) Metabolic engineering of *Klebsiella*  
508 *pneumoniae* and in silico investigation for enhanced 2,3-butanediol production. *Biotechnol Lett*  
509 38:975-982

509 Silveira MM, Schmidell W, Berbert MA (1993) Effect of the air supply on the production of 2, 3-  
510 butanediol by *Klebsiella pneumoniae* NRRL B199. *J Biotechnol* 31(1):93-102

511 Sun Y, Wei D, Shi J, Mojović L, Han Z, Hao J (2014) Two-stage fermentation for 2-ketogluconic acid  
512 production by *Klebsiella pneumoniae*. *J Microbiol Biotechnol* 24(6):781-787

513 Van Houdt R, Aertsen A, Michiels CW (2007) Quorum-sensing-dependent switch to butanediol  
514 fermentation prevents lethal medium acidification in *Aeromonas hydrophila* AH-1N. *Res*  
515 *Microbiol* 158(4):379-385

516 Wang D, Wang C, Wei D, Shi J, Kim CH, Jiang B, Han Z, Hao J (2016) Gluconic acid production by gad  
517 mutant of *Klebsiella pneumoniae*. *World J Microbiol Biotechnol* 32(8):132

518 Wang D, Zhou J, Chen C, Wei D, Shi J, Jiang B, Liu P, Hao J (2015) R-acetoin accumulation and  
519 dissimilation in *Klebsiella pneumoniae*. *J Ind Microbiol Biotechnol* 42(8):1105-1115

520 Wei D, Wang M, Shi J, Hao J (2012) Red recombinase assisted gene replacement in *Klebsiella*  
521 *pneumoniae*. *J Ind Microbiol Biotechnol* 39(8):1219-1226

522 Wei D, Xu J, Sun J, Shi J, Hao J (2013) 2-Ketogluconic acid production by *Klebsiella pneumoniae*  
523 CGMCC 1.6366. *J Ind Microbiol Biotechnol* 40(6):561-570

524 Xiao Z, Xu P (2007) Acetoin metabolism in bacteria. *Crit Rev Microbiol* 33:127–140

525 Xu YZ, Guo NN, Zheng ZM, Ou XJ, Liu HJ, Liu DH (2009) Metabolism in 1, 3-propanediol fed-batch  
526 fermentation by ad-lactate deficient mutant of *Klebsiella pneumoniae*. *Biotechnol and Bioeng*  
527 104(5):965-972

528 Zeng A-P, Biebl H, Deckwer W-D (1990) Effect of pH and acetic acid on growth and 2, 3-butanediol  
529 production of *Enterobacter aerogenes* in continuous culture. *Appl Microbiol Biotechnol*  
530 33(5):485-489

531 Zhou J, Wang D, Wang C, Gu J, Kim CH, Shi J, Jiang B, Wang M, Hao J (2017) The Role of the Pyruvate

532 Acetyl-CoA Switch in the Production of 1, 3-Propanediol by *Klebsiella pneumoniae*. Appl  
533 Biochem Biotechnol 181(3):1199-1210

534 **Figure captions**

535 Fig. 1. 2,3-Dihydroxyisovalerate synthesis related metabolic pathways. A: *K. pneumoniae* wild-type  
536 strain; B: 2,3-dihydroxyisovalerate producing strain *K. pneumoniae*  $\Delta budA-\Delta ldhA-\Delta ilvD$ .

537 Solid line: one step of reaction; dash line: contains several steps of reaction; the line thickness represent  
538 the likely metabolic flux. *ldhA*: lactate dehydrogenase; *budB*:  $\alpha$ -acetolactate synthase; *ilvBN*, *ilvGM*,  
539 *ilvIH*: acetohydroxy acid synthase; *budA*:  $\alpha$ -acetolactate decarboxylase; *ilvC*: acetohydroxy acid  
540 isomeroreductase; *ilvD*: dihydroxy acid dehydratase; *ilvE*: transaminase; *leuA*: 2-isopropylmalate  
541 synthase. The blue color genes and reactions belong to 2,3-butanediol synthesis pathway; the red color  
542 genes and reactions belong to branched-chain amino acid synthesis pathway.

543 Fig. 2. Growth and product formation of *K. pneumoniae* strains grown in batch culture on corn steep liquor  
544 free medium in shake flasks. A: Glucose; B: 2,3-dihydroxyisovalerate; C: Cell density; D: 2,3-butanediol;  
545 E: Lactic acid. F. Acetic acid. Data points are the average of n = 3; error bars represent standard error  
546 about the mean.

547 Fig. 3. Growth and product formation of *K. pneumoniae*  $\Delta budA-\Delta ldhA-\Delta ilvD$  in minimal medium with  
548 different carbon sources. A: Carbon sources; B: 2,3-dihydroxyisovalerate; C: Cell density; D: 1,3-  
549 propanediol. Data points are the average of n = 3; error bars represent standard error about the mean.

550 Fig. 4. Growth and product formation of *K. pneumoniae*  $\Delta budA-\Delta ldhA-\Delta ilvD$  in fermentation medium  
551 with different carbon sources. A: Carbon source utilization; B: 2,3-dihydroxyisovalerate; C: Cell density;  
552 D: 1,3-propanediol.

553 Fig. 5. Growth and product formation of *K. pneumoniae*  $\Delta budA-\Delta ldhA-\Delta ilvD$  in fermentation medium  
554 with different culture pH. The strain was grown in stirred tank bioreactors operated at an agitation rate  
555 of 300 rpm and an aeration rate of 2 L/min. A: Cell growth; B: Glucose; C: 2,3-Dihydroxyisovalerate; D:  
556 succinic acid; E: Acetic acid; F: Formic acid; G: Ethanol. Data points for pH 7 cultivation are the average  
557 of n = 3; error bars represent standard error about the mean.

558 Fig. 6. Growth and product formation of *K. pneumoniae*  $\Delta budA-\Delta ldhA-\Delta ilvD$  in fermentation medium  
559 (pH 7.0) with different agitation rates. The strain was grown in stirred tank bioreactors and the aeration  
560 rate set at 2 L/min. A: Cell growth; B: Glucose; C: 2,3-Dihydroxyisovalerate; D: succinic acid; E: Acetic  
561 acid; F: Formic acid; G: Ethanol. Data points for 300 rpm cultivation are the average of n = 3; error bars  
562 represent standard error about the mean.

563 Fig. 7. Growth and product formation of *K. pneumoniae*  $\Delta budA-\Delta ldhA-\Delta ilvD$  in fed batch fermentation.  
564 Cells were grown in fermentation medium (pH 6.5) in a stirred tank bioreactor operated at 400 rpm and

565 and aeration rate of 2 L/min. A: Cell growth; B: Glucose; C: 2,3-Dihydroxyisovalerate; D: succinic acid;  
566 E: Acetic acid; F: Formic acid; G: Ethanol. Data points are the average of  $n = 3$ ; error bars represent  
567 standard error about the mean.  
568

569 **Tables**

570

571 Table 1 Strains and plasmids

Strains or plasmids	Relevant genotype and description	Reference or source
<i>K. pneumoniae</i> strains		
CGMCC 1.6366	TUAC01 Wild type	(Hao et al. 2008)
$\Delta ilvD$	$\Delta ilvD$ , Apr <sup>r</sup>	This work
$\Delta budA$	$\Delta budA$ , Str <sup>r</sup>	(Wei et al. 2013)
$\Delta ldhA$	$\Delta ldhA$ , Apr <sup>r</sup>	(Gu et al. 2017)
$\Delta budA$ - $\Delta ilvD$	$\Delta budA$ , Str <sup>r</sup> , $\Delta ilvD$ , Apr <sup>r</sup>	This work
$\Delta budA$ - $\Delta ldhA$	$\Delta budA$ , Str <sup>r</sup> , $\Delta ldhA$ , Apr <sup>r</sup>	(Gu et al. 2017)
$\Delta budA$ - $\Delta ldhA$ - $\Delta ilvD$	$\Delta budA$ , Str <sup>r</sup> , $\Delta ldhA$ , $\Delta ilvD$ , Apr <sup>r</sup>	(Gu et al. 2017)
<i>E. coli</i> DH5 $\alpha$	Host of plasmid	Lab stock
plasmids		
pDK6-red	Kan <sup>r</sup> , carries $\lambda$ -Red genes (gam, bet, exo) 7.1 kbp	(Wei et al. 2012)
pDK6-flp	Kan <sup>r</sup> , carries the yeast FLP recombinase gene 6.3 kbp	(Wei et al. 2012)
pIJ790	Cm <sup>r</sup> , encodes $\lambda$ -Red genes (gam, bet, exo), 6084 bp	(Gust et al. 2003)
pIJ773	Apr <sup>r</sup> , <i>aac(3)IV</i> with FRT sites, 4334 bp	(Gust et al. 2003)
pIJ778	Str <sup>r</sup> , <i>aadA</i> with FRT sites, 4337 bp	(Gust et al. 2003)
pMD18-T	Amp <sup>r</sup> , TA cloning vector, 2,692 bp	Takara
pMD18-T- <i>ilvD</i>	Amp <sup>r</sup> , carries <i>ilvD</i>	This work
pMD18-T- <i>ilvD</i> -773	Amp <sup>r</sup> , Apr <sup>r</sup> , carries part of <i>ilvD</i>	This work
pMD18-T- <i>ilvD</i> -778	Amp <sup>r</sup> , Str <sup>r</sup> , carries part of <i>ilvD</i>	This work

572

573

574

575

576

577

578

579 Table 2 Primers

Primer name	Sequence (5'-3')
ilvD-s	GCACCGTCCCATTTAATAAAC
ilvD-a	ATGATTAGCCACCCAGTTTC
ilvD-FRT-s	CGCCGATCGTAAGGAGCTGTTTCCTTAACGCCGGGAAACGATTCCGG GGATCCGTCGACC
ilvD-FRT-a	GGTGGTACGGATGCCCGCCGGGCCGCGCGGAACATCTTTGTAGGC TGGAGCTGCTTC

580

581

582

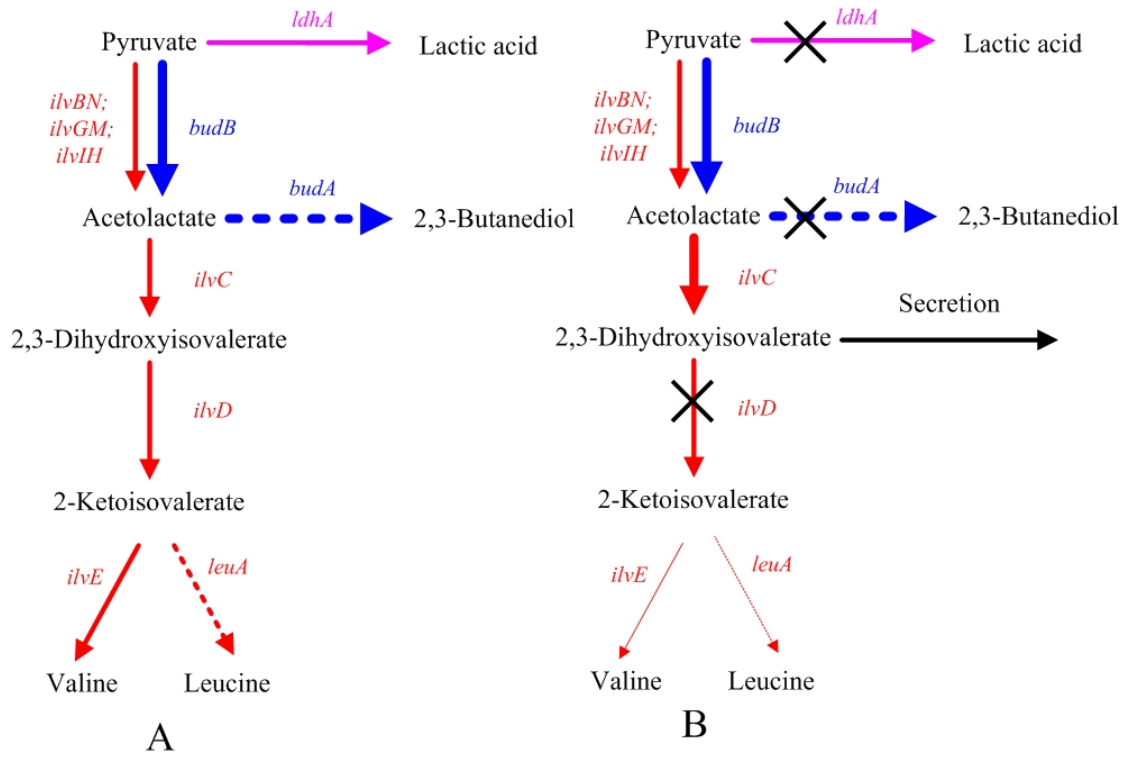
583 Table 3. <sup>1</sup>H and <sup>13</sup>C NMR chemical shift for 2,3-dihydroxyisovalerate

Hydrogen	CH	CH <sub>3</sub>	Carbon	C1	C2	C3	C4, C5
Chemical shift ppm (δ)	4.03	1.22; 1.24		176.32	77.27	72.3	24.54; 24.67

584

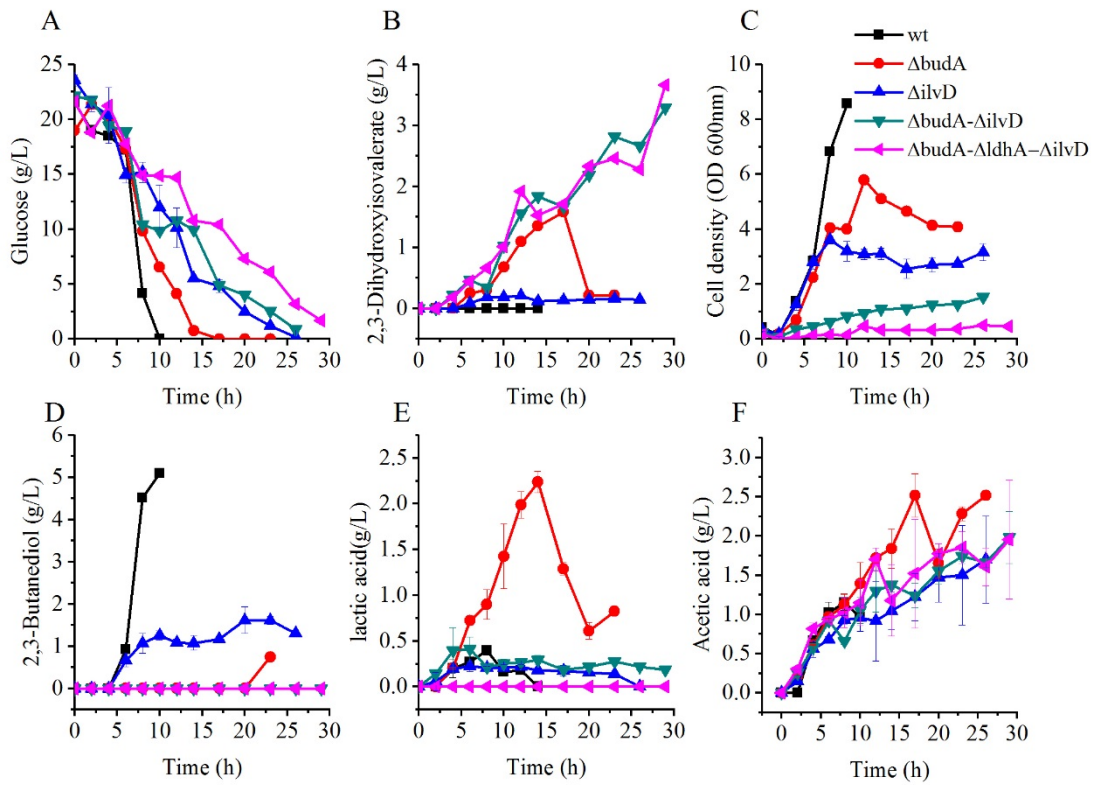
585

586



588

589 Figure 1

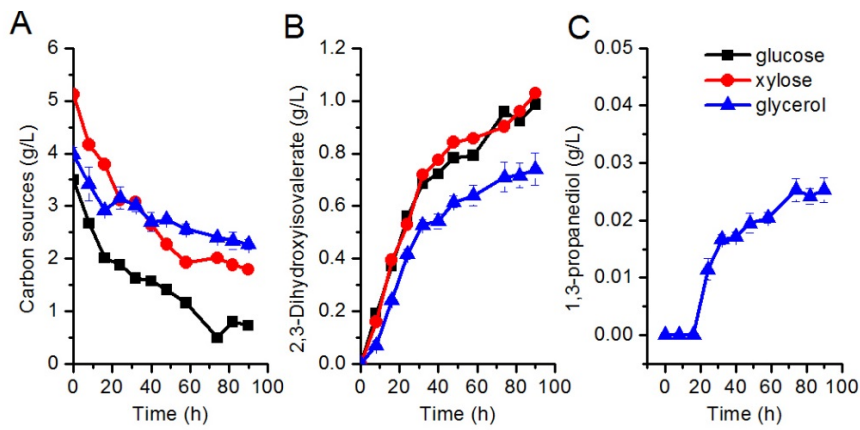


590

591

592

593 Figure 2



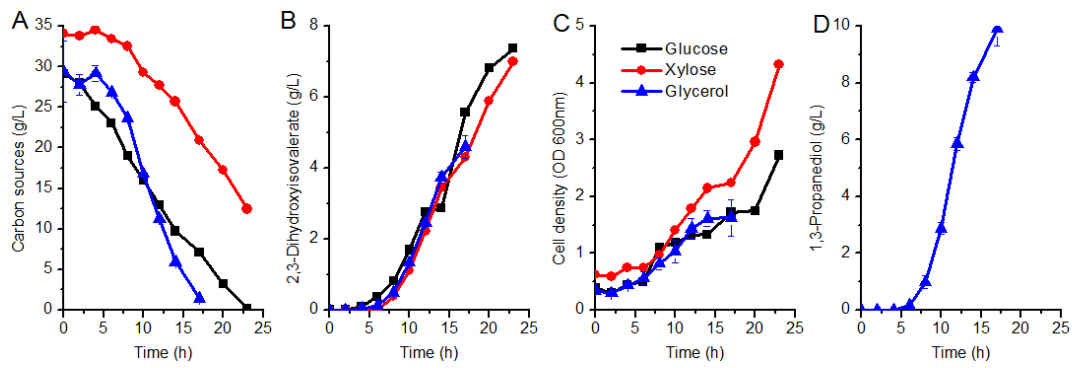
594

595 Figure 3

596

597

598

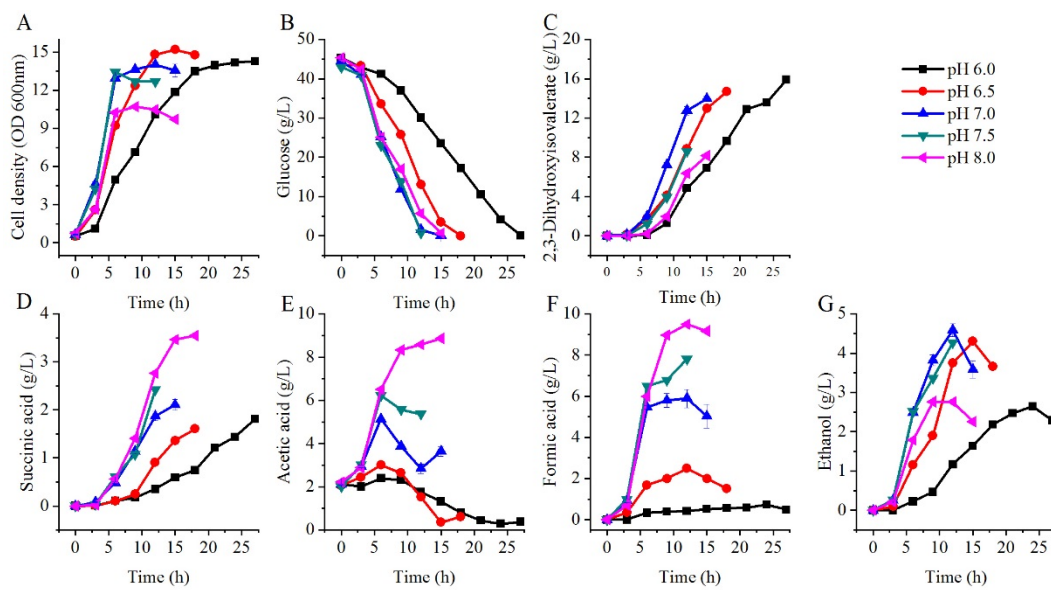


599

600 Figure 4

601

602

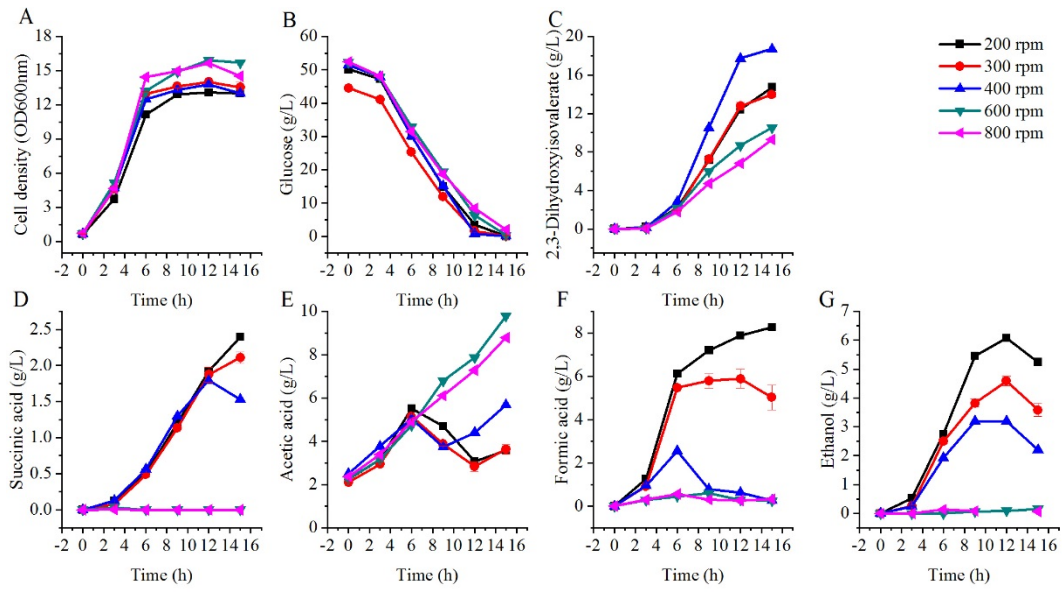


603

604 Figure 5

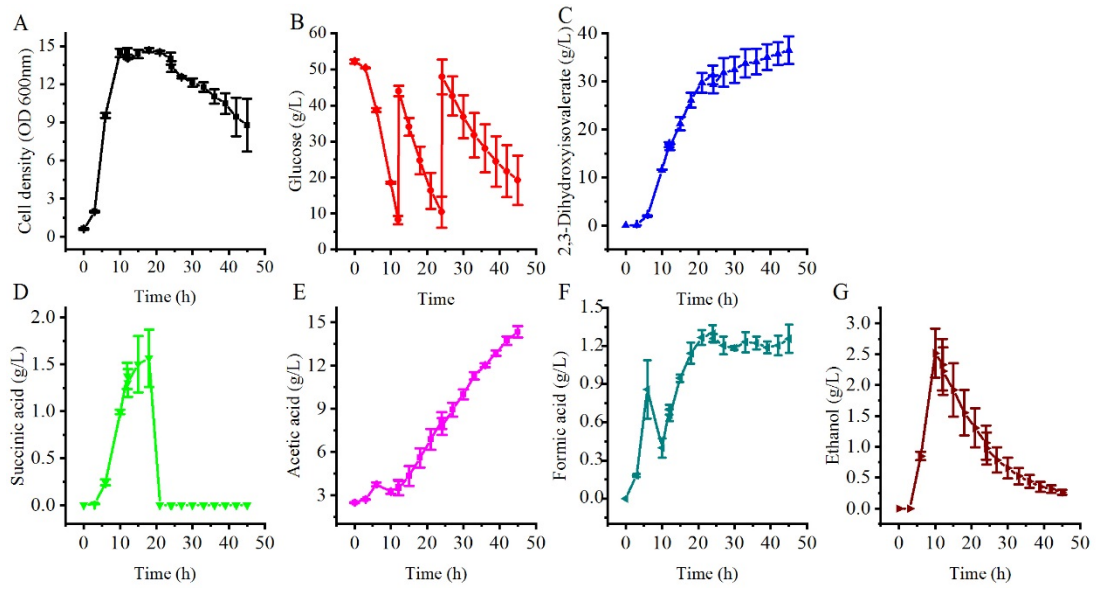


605  
606  
607



608  
609  
610  
611

Figure 6



612  
613

Figure 7